

Physical black holes in semiclassical gravity

Sebastian Murk

*Department of Physics and Astronomy, Macquarie University,
Sydney, New South Wales 2109, Australia*

and

*Sydney Quantum Academy,
Sydney, New South Wales 2006, Australia*

E-mail: sebastian.murk@mq.edu.au

Daniel R. Terno

*Department of Physics and Astronomy, Macquarie University,
Sydney, New South Wales 2109, Australia*

E-mail: daniel.terno@mq.edu.au

We derive and critically examine properties of physical black holes (PBHs) that follow from the formation of a regular apparent horizon in finite time of a distant observer. In spherical symmetry, only two distinct classes of solutions to the semiclassical Einstein equations are self-consistent. Both are required to describe PBH formation and violate the null energy condition in the vicinity of the outer horizon. The near-horizon geometry differs considerably from the one that is described by classical solutions. Accretion after horizon formation results in a firewall that violates quantum energy inequalities. Consequently, semiclassical PBHs can only evaporate once a horizon has formed. The two principal generalizations of surface gravity to dynamic spacetimes are irreconcilable, and neither can describe the emission of nearly-thermal radiation. Comparison of the required energy and timescales with established semiclassical results suggests that if the observed astrophysical black holes indeed have horizons, their formation is associated with new physics.

Keywords: black holes; general relativity; semiclassical gravity; quantum aspects of black holes; energy conditions; surface gravity.

Contribution to the proceedings of the 16th Marcel Grossmann meeting (5–10 July 2021).
Session classification: Theoretical and observational studies of astrophysical black holes

1. Introduction

Our current understanding of ultra-compact objects (UCOs) can be summarized as follows: the existence of astrophysical black holes (ABHs) — dark massive compact objects — is established beyond any reasonable doubt. However, it is unclear when, how, or if at all these UCOs develop the standard black hole features, such as horizons and singularities. A large number of models, often with deliberately designed features (or lack thereof), purport to describe ABHs. Translating the differences between these models into potentially observable differences between the signals received from the black hole candidates they describe is one of the most exciting topics in gravitational physics research^{1,2}.

There is no unanimously agreed upon definition of a black hole³. The salient

feature of a mathematical black hole (MBH)⁴ is the event horizon that separates our outside world from an inaccessible interior. However, event horizons are global teleological entities that are even in principle unobservable^{5,6}, and observational, numerical, and theoretical studies focus on other characteristics of black holes.

A trapped region is a spacetime domain where both ingoing and outgoing future-directed null geodesics emanating from a spacelike two-dimensional surface with spherical topology have negative expansion⁷⁻⁹. Its evolving outer boundary is the apparent horizon. This definition captures the most fundamental feature of black holes as spacetime regions that nothing, not even light, can escape. It is also local (and thus physically observable): the escape is not possible now, but the notion of “now” depends on the observer. Following the characterization scheme of Ref. 4, we refer to a trapped spacetime region as a physical black hole (PBH).

Further qualifications are in order. Two natural (and almost unavoidable) assumptions — regularity of the apparent horizon and its finite-time formation according to the clock of a distant observer — allow us to obtain the restricted form of the near-horizon geometry. In spherical symmetry (to which we mostly restrict our discussion here), they uniquely determine the formation scenario for PBHs. We now outline the motivation and justification for these requirements. Fig. 1 illustrates some of the considerations that underpin them.

In classical general relativity (GR) non-spacelike singularities destroy predictability. According to the weak cosmic censorship conjecture^{13,14} (which is the idea that we essentially follow here), spacetime singularities are covered by event horizons. Quantum gravitational effects are expected to become important when the spacetime curvature is sufficiently strong,^{8,15} i.e. when the Kretschmann scalar $\mathcal{K} := R_{\mu\nu\rho\sigma}R^{\mu\nu\rho\sigma}$ reaches the Planck scale, that is $\mathcal{K} \gtrsim l_{\text{P}}^{-4}$. The most spectacular prediction of quantum field theory on curved backgrounds¹⁵ is Hawking radiation. It not only completed black hole thermodynamics^{8,16}, but has given rise to the infamous information loss problem¹⁰. Regular (singularity-free) black holes were introduced to altogether eliminate singularities in classical gravitational collapse or as a way to resolve the problem of information loss^{4,17,18}. Leaving aside discussions of cosmic censorship, we formulate the regularity criterion as the absence of singularities at the apparent horizon. A precise mathematical formulation is provided in Sec. 2.

For a horizon to be considered a genuine physical object rather than merely a useful mathematical tool, it must form in finite time of a distant observer, and there should be some potentially observable consequences of this formation. Moreover, if black holes do indeed emit Hawking radiation, and their evolution roughly resembles that of Fig. 1(a), then the apparent horizon forms in finite time t_{S} of a distant observer. We note that, as illustrated in Fig. 1(a), the outer apparent horizon is located outside of the event horizon^{8,10}. Hence all signals that are emitted from the so-called quantum ergosphere^{12,19} — part of the trapped region that lies outside of the event horizon — reach future null infinity \mathcal{I}^+ . Moreover, models of transient

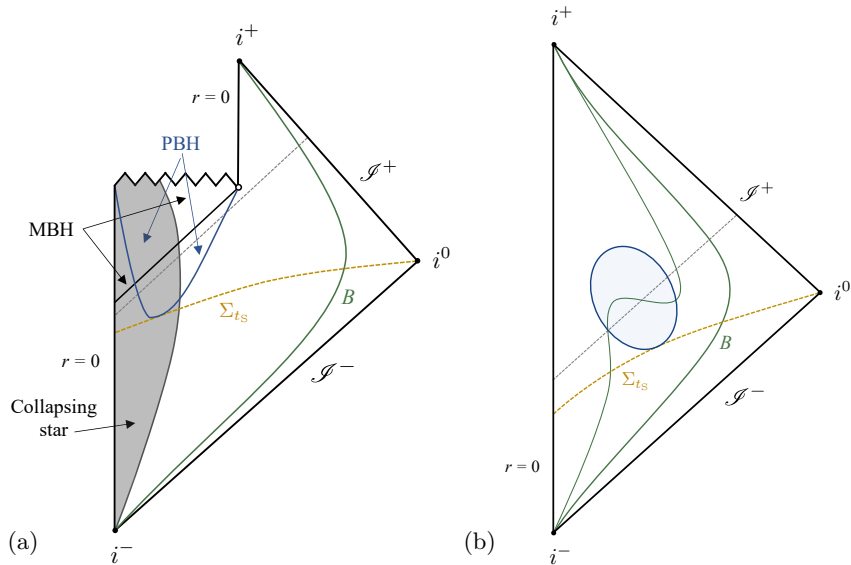


Fig. 1. Schematic Carter–Penrose diagram of (a) the conventional formation and evaporation of a black hole, and (b) the formation and evaporation of a RBH. The outer apparent horizon $r_g(t)$ and the inner apparent horizon $r_{in}(t)$ form the boundary of a PBH and are shown in blue. The equal time surface Σ_{t_S} is drawn as a dashed orange line. The trajectory of a distant observer Bob is labeled “B” and indicated in green. Dashed grey lines correspond to outgoing radial null geodesics. (a) Diagrams of this type are elaborations of the original sketch by Hawking¹⁰. Spacetime regions corresponding to PBH (MBH) solutions are indicated by blue (black) arrows. Light signals emitted from within the trapped region, but outside of the event horizon, reach \mathcal{I}^+ and are detected by Bob in his finite proper time. The collapsing matter and its surface are shown as in conventional depictions of the collapse. However, the matter in the vicinity of the outer apparent horizon $(t, r_g(t))$ violates the NEC for $t \geq t_S$. Moreover, the energy density, pressure, and flux as seen by an infalling observer Alice vary continuously across it, and the equation of state dramatically differs from that of normal matter that may have been used to model the initial EMT of the collapse. (b) The asymptotic structure of a simple RBH spacetime¹¹ coincides with that of Minkowski spacetime. Conditions for the smooth joining of the inner and outer apparent horizon are described in Ref. 12. An unmarked green line represents a hypersurface $r = \text{const}$ that passes through the PBH.

(even if long-lived) regular black holes (RBHs) imply the finite-time formation and disappearance of the trapped region, as depicted in Fig. 1(b). This leads to our second requirement: the finite-time formation of an apparent horizon according to a distant observer.

Working in the framework of semiclassical gravity, we use classical notions (horizons, trajectories, etc.) and describe dynamics via the Einstein equations $G_{\mu\nu} = 8\pi T_{\mu\nu}$. We do not assume any specific matter content nor a specific quantum state ω that produces the expectation values of the energy-momentum tensor (EMT) $T_{\mu\nu} = \langle \hat{T}_{\mu\nu} \rangle_\omega$. Note that this EMT describes the total matter content — both the original collapsing matter and the produced excitations. We do not

assume the presence of Hawking-like radiation, an event horizon, or a singularity. To simplify the exposition we work in asymptotically flat spacetimes, even if it is not essential for the resulting near-horizon geometries.

2. Admissible spherically symmetric solutions

It is convenient to use Schwarzschild coordinates to impose the two assumptions described above. Here, the time t represents the physical time of a stationary distant observer, and the coordinate singularities allow us to identify the admissible solutions. A general spherically symmetric metric is given by

$$ds^2 = -e^{2h(t,r)} f(t,r) dt^2 + f(t,r)^{-1} dr^2 + r^2 d\Omega. \quad (1)$$

These coordinates provide geometrically preferred foliations with respect to Kodama time, a natural divergence-free preferred vector field^{9,20}. Using the advanced null coordinate v , the metric is written as

$$ds^2 = -e^{2h_+} \left(1 - \frac{C_+}{r}\right) dv^2 + 2e^{h_+} dv dr + r^2 d\Omega. \quad (2)$$

The Misner–Sharp (MS) mass^{9,21} $C(t, r)/2$ is invariantly defined via

$$f(t, r) := 1 - C/r := \partial_\mu r \partial^\mu r, \quad (3)$$

and thus $C(t, r) \equiv C_+(v(t, r), r)$. The functions $h(t, r)$ and $h_+(v, r)$ play the role of integrating factors in coordinate transformations, such as

$$dt = e^{-h} (e^{h_+} dv - f^{-1} dr). \quad (4)$$

The apparent horizon is located at the Schwarzschild radius $r_g(t) \equiv r_+(v)$ that is the largest root of $f(t, r) = 0$ ^{9,22}. In (v, r) coordinates the tangents to the ingoing and outgoing radial geodesics are given by

$$l_{\text{in}}^\mu = (0, -e^{-h_+}, 0, 0), \quad l_{\text{out}}^\mu = (1, \frac{1}{2}e^{h_+} f, 0, 0), \quad (5)$$

respectively. They are normalized to satisfy $l_{\text{in}} \cdot l_{\text{out}} = -1$, and their corresponding expansions are

$$\vartheta_{\text{in}} = -\frac{e^{-h_+}}{r}, \quad \vartheta_{\text{out}} = \frac{e^{h_+} f}{r}. \quad (6)$$

The Schwarzschild coordinates become singular as $r \rightarrow r_g$. We extract information about the EMT and therefore about the near-horizon geometry by studying how various divergences cancel to produce finite curvature scalars. Singular points are identified through the presence of incomplete geodesics in their vicinity and are excluded from manifolds representing the spacetime. These geodesics are inextendible in at least one direction, but the range of their generalized affine parameter (proper time for timelike geodesics) is bounded^{7,14,23,24}. We focus on curvature singularities and formalize the regularity requirement as the demand that curvature scalars built from polynomials of Riemann tensor components are finite. This condition

corresponds to the absence of essential scalar curvature singularities. More stringent conditions that involve higher covariant derivatives or regularity of individual components are not imposed.

In a general four-dimensional spacetime, there are 14 algebraically independent scalar invariants that can be constructed from the Riemann tensor²⁵. We use two quantities that are expressed straightforwardly from components of the EMT, namely

$$\tilde{\mathbb{T}} := T^\mu{}_\mu, \quad \tilde{\mathfrak{T}} := T_{\mu\nu} T^{\mu\nu}. \quad (7)$$

The Einstein equations relate them to the curvature scalars as $\tilde{\mathbb{T}} \equiv -\mathcal{R}/8\pi$ and $\tilde{\mathfrak{T}} \equiv R^{\mu\nu} R_{\mu\nu}/64\pi^2$, where $R_{\mu\nu}$ and \mathcal{R} are the Ricci tensor and Ricci scalar, respectively. In spherical symmetry, if the two scalars of Eq. (7) are finite, then the rest are finite as well²⁶.

It is convenient to introduce

$$\tau_t := e^{-2h} T_{tt}, \quad \tau_t{}^r := e^{-h} T_t{}^r, \quad \tau^r := T^{rr}. \quad (8)$$

The three Einstein equations for G_{tt} , $G_t{}^r$, and G^{rr} can then be written as

$$\partial_r C = 8\pi r^2 \tau_t / f, \quad (9)$$

$$\partial_t C = 8\pi r^2 e^h \tau_t{}^r, \quad (10)$$

$$\partial_r h = 4\pi r (\tau_t + \tau^r) / f^2. \quad (11)$$

Since the term $T^\theta{}_\theta \equiv T^\varphi{}_\varphi$ is finite in GR^{27,28}, regularity of the apparent horizon requires that the scalars

$$\mathbb{T} = (\tau^r - \tau_t) / f, \quad \mathfrak{T} = ((\tau^r)^2 + (\tau_t)^2 - 2(\tau_t{}^r)^2) / f^2, \quad (12)$$

are finite at $r = r_g$. It was shown that only two classes of dynamic solutions (with the leading terms in the functions τ_a , $a \in \{t, t{}^r, r\}$ scaling as f^k , $k = 0, 1$) satisfy the regularity conditions^{28,29}. We now briefly summarize their properties.

2.1. Generic solution ($k = 0$)

In principle, the solutions with $k = 0$ allow for $\tau_t \rightarrow \tau^r \rightarrow \mp \Upsilon^2$, $\tau_t{}^r \rightarrow \mp \Upsilon^2$ for some $\Upsilon(t) > 0$, but only

$$\tau_t \approx \tau^r = -\Upsilon^2 + \mathcal{O}(\sqrt{x}), \quad (13)$$

$$\tau_t{}^r = -\Upsilon^2 + \mathcal{O}(\sqrt{x}), \quad (14)$$

where $x := r - r_g$ denotes the coordinate distance from the horizon, describe valid PBH solutions: taking $\tau_t \rightarrow \tau^r \rightarrow +\Upsilon^2$ results in complex-valued solutions of Eqs. (9)–(11) (see Ref. 27 for details). The negative sign in the leading term of τ_t and τ^r leads to the violation of the null energy condition (NEC)^{7,30,31} in the vicinity of the apparent horizon, i.e. a future-directed outward (inward) pointing radial null vector k^μ does not satisfy $T_{\mu\nu} k^\mu k^\nu \geq 0$ for the contracting (expanding) Schwarzschild radius r_g ²⁷. An immediate consequence of this result is that accreting

Vaidya black hole solutions in (v, r) coordinates cannot describe PBHs as they satisfy the NEC²⁷.

The metric functions that solve Eq. (9) and Eq. (11) are

$$\begin{aligned} C &= r_g - 4\sqrt{\pi}r_g^{3/2}\Upsilon\sqrt{x} + \mathcal{O}(x), \\ h &= -\frac{1}{2}\ln\frac{x}{\xi} + \mathcal{O}(\sqrt{x}), \end{aligned} \quad (15)$$

where $\xi(t)$ is determined by the choice of time variable and the higher-order terms depend on the higher-order terms in the EMT expansion³². Eq. (10) must then hold identically. Both sides contain terms that diverge as $1/\sqrt{x}$, and their identification results in the consistency condition

$$r'_g/\sqrt{\xi} = \mp 4\sqrt{\pi r_g}\Upsilon, \quad (16)$$

where the minus (plus) sign corresponds to evaporation (accretion). Useful information can be obtained by working with retarded and advanced null coordinates that result in regular metric functions²⁷. If $r'_g > 0$, this is achieved by using the retarded null coordinate u . For $r'_g < 0$, the advanced null coordinate v leads to

$$C_+(v, r) = r_+(v) + \sum_{i \geq 1} w_i(v)(r - r_+)^i, \quad (17)$$

$$h_+(v, r) = \sum_{i \geq 1} \chi_i(v)(r - r_+)^i, \quad (18)$$

for some functions $w_i(v)$, $\chi_i(v)$, where $w_1 \leq 1$ due to the definition of r_+ . This is the general form of the metric functions in (v, r) coordinates that ensures finite curvature scalars at the apparent horizon if $r'_g < 0$ ²⁸. The components of the EMT in (v, r) and (t, r) coordinates are related by

$$\theta_v := e^{-2h_+}\Theta_{vv} = \tau_t, \quad (19)$$

$$\theta_{vr} := e^{-h_+}\Theta_{vr} = (\tau_t{}^r - \tau_t)/f, \quad (20)$$

$$\theta_r := \Theta_{rr} = (\tau^r + \tau_t - 2\tau_t{}^r)/f^2, \quad (21)$$

where $\Theta_{\mu\nu}$ labels the EMT components in (v, r) coordinates.

The limiting form of the (tr) block of the EMT as $r \rightarrow r_g$ is

$$T^a_b = \begin{pmatrix} \Upsilon^2/f & -\varepsilon_{\pm}e^{-h}\Upsilon^2/f^2 \\ \varepsilon_{\pm}e^h\Upsilon^2 & -\Upsilon^2/f \end{pmatrix}, \quad T_{\hat{a}\hat{b}} = \frac{\Upsilon^2}{f} \begin{pmatrix} -1 & \varepsilon_{\pm} \\ \varepsilon_{\pm} & -1 \end{pmatrix}, \quad (22)$$

where the second expression is written in the orthonormal frame. It makes the violation of the NEC particularly transparent.

In the test-field limit¹⁵ quantum fields propagate on a given gravitational background, but the resulting EMT is not permitted to backreact on the geometry via the Einstein equations. It is instructive to compare the tensor of Eq. (22) with explicit results obtained in the test-field limit. Out of the three popular choices for the vacuum state^{8,15}, only the Unruh vacuum results in an EMT with nonzero

T_{tr} components. The state itself corresponds to the requirement that no particles impinge on the collapsing object from infinity³³. In the context of a static maximally extended spacetime, its counterpart is a state with unpopulated modes at past null infinity and the white hole horizon^{8,15}. Using various semi-analytical and numerical methods that are based on conformally coupled fields³⁴ and minimally coupled scalar field³⁵, the expectation values of the renormalized components T_{tt} , T_t^r , and T^{rr} have been determined explicitly. They approach the same negative value as $r \rightarrow r_g$.

The experiences of observers in the vicinity of the apparent horizon depend on their trajectories. A static observer finds that the energy density $\rho := T_{\mu\nu} u^\mu u^\nu = -T_t^t$, pressure $p := T_{\mu\nu} n^\mu n^\nu = T_r^r$, and flux $\phi := T_{\mu\nu} u^\mu n^\nu$, where u^μ denotes the four-velocity and n^μ the outward-pointing radial spacelike vector, diverge at the apparent horizon. The experience of a radially-infalling observer Alice moving on the trajectory $x_A^\mu(\tau) = (t_A, r_A, 0, 0)$ is different, and also differs from the infall into a classical eternal black hole.

First, horizon crossing happens not only at some finite proper time τ_0 , but also at a finite time $t_0(\tau_0)$, $r_g(t_0(\tau_0)) = r_A(\tau_0)$ according to the clock of a distant Bob. This is particularly easy to see for ingoing null geodesics, where

$$\frac{dt}{dr} = -\frac{e^{-h(t,r)}}{f(t,r)} \rightarrow \pm \frac{1}{r'_g}, \quad (23)$$

at $r = r_g$, the rhs is obtained using Eqs. (15) and (16)²⁸, and the upper signature corresponds to evaporation. We use this result in our estimate of the formation time in Sec. 4, and in showing that the usual generalizations of surface gravity to nonstationary spacetimes fail for PBHs (Sec. 3.2).

For an evaporating black hole ($r'_g < 0$), energy density, pressure, and flux in Alice's frame are finite. However, upon crossing the apparent horizon of an accreting PBH, Alice encounters a firewall,

$$\rho_A = T_{\mu\nu} u_A^\mu u_A^\nu = -\frac{\dot{r}_A^2}{4\pi r_g X} + \mathcal{O}(1/\sqrt{X}), \quad (24)$$

where $X := r_A(\tau) - r_g(t_A(\tau))$ ²⁶.

Violations of the NEC are bounded by quantum energy inequalities^{31,36}. Outside of the singularities the lower bounds were shown to exist for the energy density $\langle \hat{T}_{\mu\nu} \rangle_\omega u^\mu u^\nu$ and its smeared averages. These are known to be state-independent for free fields. For spacetimes of small curvature, explicit bounds for a geodesic observer were derived in Ref. 37. A finite bound is violated by the $1/f^2$ divergence of the energy density that results in the logarithmic divergence of its smeared time average^{28,38}. Thus we are faced with the following conundrum: either accretion to a UCO can only occur before the first marginally trapped surface appears, and PBHs, once formed, can only evaporate, or semiclassical physics breaks down at the horizon scale. Therefore, we restrict our discussion to evaporating PBHs in what follows.

Observers that have crossed the apparent horizon but change their mind before traversing the quantum ergosphere can exit the black hole before it evaporates. Their experiences at the apparent horizon are more involved: for a geodesic observer that attempts to cross the apparent horizon from the inside, the energy density also diverges. However, it does so according to a weaker $1/f$ law and thus the integrated energy density remains finite.

It is possible to find explicit relations between (t, r) and (v, r) coordinates in the vicinity of the apparent horizon^{29,39}, namely

$$x(r_+ + y, v) = r_+ + y - r_g(t(v, r_+ + y)) = -r_g'' y^2 / (2r_g'^2) + \mathcal{O}(y^3), \quad (25)$$

which relates the coordinates $x = r - r_g(t)$ and $y(r, v) := r - r_+(v)$. Another useful relation is

$$w_1 = 1 - 2\sqrt{2\pi r_g^3 |r_g''|} \frac{\Upsilon}{|r_g'|}. \quad (26)$$

2.2. Extreme solution ($k = 1$)

The static solution with $k = 0$ is impossible, as in this case \mathfrak{T} would diverge at the apparent horizon. Consequently, EMT components that allow for static solutions must behave differently. Many models of static nonsingular black holes assume finite values of energy density and pressure at the horizon^{4,18}. With respect to the scaling behavior f^k of the invariants of Eq. (12), this is the $k = 1$ solution, with

$$\tau_t \rightarrow E(t)f, \quad \tau_t^r \rightarrow \Phi(t)f, \quad \tau^r \rightarrow P(t)f, \quad (27)$$

where $\rho = E$ and $p = P$ at the apparent horizon. Any two functions can be expressed algebraically in terms of the third, and $8\pi r_g^2 E \leq 1$ to ensure that $C(t, r) - r_g > 0$ for $r > r_g$.

Only the extreme value of $E = (8\pi r_g^2)^{-1}$ corresponds to non-extreme dynamic black holes (i.e. those with $r_g \neq \text{const}$ whose trapped regions have nonzero volume)²⁹. As a result

$$C(t, r) = r - c_{32}(t)x^{3/2} + \mathcal{O}(x^2), \quad (28)$$

for some coefficient $c_{32}(t) > 0$, setting via Eq. (27) the scaling of other leading terms in the EMT. The consistency of Eqs. (10) and (11) implies $P = -E = -1/(8\pi r_g^2)$ and $\Phi = 0$. From the next-order expansion we obtain

$$h = -\frac{3}{2} \ln \frac{x}{\xi} + \mathcal{O}(\sqrt{x}), \quad (29)$$

as well as the consistency relation

$$r_g' = -c_{32}\xi^{3/2}/r_g. \quad (30)$$

The NEC violation is more subtle than in the $k = 0$ case. At $r = r_g(t)$ itself the NEC is marginally satisfied, as

$$T_{\hat{a}\hat{b}} = \frac{1}{8\pi r_g^2} \begin{pmatrix} 1 & 0 \\ 0 & -1 \end{pmatrix}. \quad (31)$$

However, the NEC is violated for some $x > 0$, as for both incoming and outgoing directions $l_{\text{in}}, l_{\text{out}}$ we have

$$T_{\hat{a}\hat{b}} l^{\hat{a}} l^{\hat{b}} = -\frac{3c_{32}\sqrt{x}}{8\pi r_g^2} + \mathcal{O}(x). \quad (32)$$

Solutions with a time-independent apparent horizon or general static solutions do not require $w_1 = 1$ to satisfy Eqs. (19)–(21). Since $r_+(v) = r_g(t) = \text{const}$, it is possible to have non-extreme solutions. Then Eq. (10) implies $\Phi = 0$ and the identity $E = -P$ follows from Eq. (21), leading to a regular function $h(t, r)$. However, in this case Eq. (4) indicates that the apparent horizon cannot be reached in finite time t .

3. Implications

PBHs have many remarkable properties. First, we mention an immediate mathematical consequence of the firewalls at the apparent horizon that we have described. The divergence of ρ_A (see Eq. (24)) indicates the presence of a matter singularity. As a result, we observe that if an apparent horizon forms, it is a surface with an intermediate singularity. The appearance of a negative energy firewall is the counterpart to arbitrarily large tidal forces that could tear apart an observer falling into such a singularity. In these cases the fate of an observer depends on the integrated tidal stress^{8,40}.

Since all curvature scalars remain finite it is instructive to check the Ricci spinors

$$\Phi_{00} = \frac{1}{2}R_{11}, \quad \Phi_{22} = \frac{1}{2}R_{22}, \quad \Phi_{11} = \frac{1}{4}(R_{12} + R_{34}). \quad (33)$$

Using the natural Newman–Penrose tetrad that is built from the two null vectors of Eq. (5) and a pair of complex-conjugate vectors m^μ and $\bar{m}^\mu := m^{\mu*}$,

$$m = \frac{1}{\sqrt{2}r} \partial_\theta + \frac{i}{\sqrt{2}r \sin \theta} \partial_\phi, \quad m \cdot \bar{m} = 1, \quad (34)$$

we find that the values of all nonzero spinors are finite at the apparent horizon. However, given the freedom of choice of these vectors $l_{\text{out}}^\mu \rightarrow A l_{\text{out}}^\mu$, $l_{\text{in}}^\mu \rightarrow l_{\text{in}}^\mu / A$, the values of the spinors Φ_{00} and Φ_{22} depend on this choice. By choosing $A = f(v, r)$ (this form of the tangent vectors may appear more natural in (t, r) coordinates), we find

$$\Phi_{00} \propto f, \quad \Phi_{22} \propto f^{-1}, \quad (35)$$

again demonstrating that the apparent horizon is a surface of intermediate singularity³⁸.

3.1. Black hole formation

Consider now possibilities for horizon formation. The properties of the self-consistent solutions of the Einstein equations that we have described above lead

to the identification of a unique scenario for black hole formation^{28,29}. Again, we consider only evaporating ($r'_g < 0$) PBHs due to the implications of the results presented in Sec. 2.1. Working in (v, r) coordinates, we assume that the first marginally trapped surface appears at some v_S at $r_+(v_S)$ that corresponds to a finite value of t_S . For $v \leq v_S$, the MS mass in its vicinity can be described by modifying Eq. (17) as

$$C(v, r) = \Delta(v) + r_*(v) + \sum_{i \geq 1} w_i(v)(r - r_*)^i, \quad (36)$$

where $r_*(v)$ corresponds to the maximum of $\Delta_v(r) := C(v, r) - r$, and the deficit function $\Delta(v) := C(v, r_*) - r_*(v) \leq 0$. At the advanced time v_S the location of the maximum corresponds to the first marginally trapped surface, $r_*(v_S) = r_+(v_S)$, and $\sigma(v_S) = 0$. For $v \geq v_S$ the MS mass is described by Eq. (17). For $v \leq v_S$, the (local) maximum of $\Delta_v(r)$ is determined by $\Delta_v(r)/dr = 0$, hence $w_1(v) - 1 \equiv 0$.

There are no *a priori* restrictions on the evolution of r_* before the PBH is formed. However, since an accreting PBH leads to a firewall and we consider only evaporating black holes, $r'_+(v_S) < 0$. For $v > v_S$, the maximum of $C(v, r)$ does not coincide with $r_+(v)$ since the trapped region is of finite size. As a result, $w_1(v) < 1$ for $v > v_S$.

This means that at its formation a PBH is described by a $k = 1$ solution, which can be seen from Eq. (26), as $w_1 = 1$ implies $\Upsilon = 0$. It then immediately switches to the $k = 0$ solution, with matching decrease in $w_1(v)$ and increase in $\Upsilon(t(v, r_+))$, and $w_1 < 1$ at all subsequent stages. The transition from f^1 to f^0 behavior is continuous as $\Upsilon(t_S) \equiv 0$ for the $k = 1$ solution and it increases thereafter²⁹.

3.2. Surface gravity

The surface gravity κ plays an important role in GR and semiclassical gravity⁷⁻⁹. However, it is unambiguously defined only in stationary spacetimes (for a Schwarzschild black hole $\kappa = (2r_g)^{-1}$), where it is proportional to the Hawking temperature.

Generalizations of surface gravity to dynamic spacetimes are related to two equivalent definitions of κ in stationary spacetimes that are based on the peeling off properties of null geodesics near the horizon, and the inaffinity of null geodesics at the horizon, respectively^{9,41}. For sufficiently slowly evolving horizons with properties sufficiently close to their classical counterparts, these different generalizations of surface gravity are practically indistinguishable⁴¹. This agreement is important. Emission of Hawking-like radiation does not require the formation of an event or even an apparent horizon⁴²⁻⁴⁵. The role of the Hawking temperature is captured in various derivations either by the peeling⁴⁶ or the Kodama⁴⁷ surface gravity.

For PBHs, however, these quantities are very different. The peeling surface gravity κ_{peel} is defined from the near-horizon behavior of null geodesics^{9,41} as the

linear coefficient in the Taylor expansion of

$$\frac{dr}{dt} = \pm e^h f(t, r) \quad (37)$$

in powers of x as $x \rightarrow 0$ (i.e. $r \rightarrow r_g$). However, such an expansion is impossible for the metric functions of Eqs. (17)–(18). Alternatively, to be compatible with Eq. (23), κ_{peel} should be infinite, as we now demonstrate.

For differentiable C and h , the result is

$$\kappa_{\text{peel}} = \frac{e^{h(t, r_g)} (1 - C'(t, r_g))}{2r_g}. \quad (38)$$

This quantity is undefined for $k = 0$ solutions as for a radial geodesic (Eq. (23)) it implies

$$\frac{dr}{dt} = \pm |r'_g| + \mathcal{O}(\sqrt{x}), \quad (39)$$

and κ_{peel} diverges (for both $k = 0$ and $k = 1$ solutions)²⁹.

The Kodama vector field has many useful properties of the Killing field to which, modulo possible rescaling, it reduces in the static case^{9,20,41}. Similar to the Killing vector, it is most conveniently expressed in (v, r) coordinates,

$$K^\mu = (e^{-h_+}, 0, 0, 0). \quad (40)$$

It is covariantly conserved, and generates the conserved current

$$\nabla_\mu K^\mu = 0, \quad (41)$$

$$\nabla_\mu J^\mu = 0, \quad J^\mu := G^{\mu\nu} K_\nu, \quad (42)$$

thereby giving a natural geometric meaning to the Schwarzschild coordinate time t . The MS mass is its Noether charge.

Since $K_{(\mu;\nu)} \neq 0$, the generalized Hayward–Kodama surface gravity is defined via⁴⁸

$$\frac{1}{2} K^\mu (\nabla_\mu K_\nu - \nabla_\nu K_\mu) := \kappa_K K_\nu, \quad (43)$$

evaluated on the apparent horizon. Hence

$$\kappa_K = \frac{1}{2} \left(\frac{C_+(v, r)}{r^2} - \frac{\partial_r C_+(v, r)}{r} \right) \Big|_{r=r_+} = \frac{(1 - w_1)}{2r_+}, \quad (44)$$

where Eq. (17) was used to obtain the final result. Thus at the formation of a black hole (i.e. of the first trapped surface) this version of surface gravity is zero. At the subsequent evolution stages that correspond to a $k = 0$ solution, κ_K is nonzero. However, it approaches the static value $\kappa = 1/(4M)$ only if the metric is close to the pure Vaidya metric with $w_1 \equiv 0$. This in turn contradicts the semiclassical results³⁹.

4. Discussion

We have derived properties of PBHs that follow from commonly obtained or assumed, but not always sufficiently articulated requirements: the formation of a regular apparent horizon in finite time of a distant observer. The two classes of spherically symmetric solutions that satisfy these requirements must violate the NEC in the vicinity of the outer apparent horizon, and the matter content is dominated by a null fluid. Unless we accept that semiclassical physics breaks down at the horizon scale, accretion is no longer possible after the horizon has formed. This is due to the presence of a firewall that violates bounds on the violation of the NEC. The firewall is not an artifact of spherical symmetry: the same scenario occurs in Kerr–Vaidya spacetimes⁴⁹.

It is still not clear how the collapsing matter actually behaves, and how the continuous transition from f^1 to f^0 behavior upon PBH formation (Sec. 3.1) can be realized in nature. A mechanism that converts the original matter into the exotic matter present in the vicinity of the forming apparent horizon is required to violate the NEC, thus creating something akin to a shock wave to restore the normal behavior near the inner horizon. However, the emission of collapse-induced radiation^{42–44} is a nonviolent process that approaches at latter times the standard Hawking radiation and Page’s evaporation law^{8,50} $r'_g = -\alpha/r_g^2$, $\alpha \sim 10^{-3} - 10^{-4}$.

In addition, there is no obvious way to reconcile the two standard definitions of surface gravity that underpin different derivations of Hawking radiation to dynamic spacetimes (Sec. 3.2): the peeling surface gravity κ_{peel} diverges, whereas the Kodama surface gravity κ_K is zero at the instant of PBH formation and in contradiction with established semiclassical results thereafter. This has interesting repercussions for the formulation of the information loss paradox³⁹ and indicates that the Hawking radiation that is obtained on the Schwarzschild background is not an asymptotic form of the radiation that is emitted by a PBH.

Our results indicate that the observed ABHs may be horizonless UCOs rather than genuine PBHs with horizon — not due to some exotic supporting matter or dramatic variation in the laws of gravity, but simply because the conditions for the formation of a horizon have not been met at the present moment of t . Even if no new physics is required to produce the mandatory NEC violation, the process may be too slow to transform the UCOs that we observe into PBHs. Eq. (23) of Sec. 2.1 sets the timescale of the last stages of infall according to Bob. Assuming that it is applicable through the radial interval of the order of r_g , we find $t_{\text{in}} \sim r_g/r'_g$. For an evaporating macroscopic PBH, this is of the same order of magnitude as the Hawking process decay time $t_{\text{evp}} \sim 10^3 r_g^3$. Such behavior was found in thin shell collapse models, where the exterior geometry is modeled by a pure outgoing Vaidya metric³². For a solar mass black hole, this time is about 10^{64} yr, indicating that it is simply too early for the horizon to form. It is also conceivable that the conditions are not met before evaporation is complete or before effects of quantum gravity become dominant⁸. Horizon avoidance may therefore occur due to the absence of

new physics, and not because of it.

A more detailed understanding of the near-horizon geometry as well as the behavior of matter during gravitational collapse and PBH formation is needed to resolve all of the remaining questions. Coming of age of multimessenger astronomy and controversies surrounding the direct observation of ABHs make it a particularly timely project.

Acknowledgments

SM is supported by an International Macquarie University Research Excellence Scholarship and a Sydney Quantum Academy Scholarship. The work of DRT is supported by the ARC Discovery project grant DP210101279.

References

1. L. Barack, V. Cardoso, S. Nissanke, and T. P. Sotiriou (eds.), *Class. Quantum Gravity* **36**, 143001 (2019).
2. V. Cardoso and P. Pani, *Living Rev. Relativ.* **22**, 4 (2019).
3. E. Curiel, *Nat. Astr.* **3**, 27 (2019).
4. V. P. Frolov, *J. High Energy Phys.* **05**, 049 (2014).
5. M. Visser, *Phys. Rev. D* **90**, 127502 (2014).
6. V. Cardoso and P. Pani, *Nat. Astron.* **1**, 586 (2017).
7. S. W. Hawking and G. F. R. Ellis, *The Large Scale Structure of Space-Time* (Cambridge University Press, 1973).
8. V. P. Frolov and I. D. Novikov, *Black Hole Physics: Basic Concepts and New Developments* (Kluwer, Dordrecht, 1998).
9. V. Faraoni, *Cosmological and Black Hole Apparent Horizons* (Springer, Heidelberg, 2015).
10. S. W. Hawking, *Commun. Math. Phys.* **43**, 199 (1975).
11. R. Carballo-Rubio, F. Di Filippo, S. Liberati, and M. Visser, *Phys. Rev. D* **101**, 084047 (2020).
12. P. Binétruy, A. Helou and F. Lamy, *Phys. Rev. D* **98**, 064058 (2018).
13. J. M. M. Senovilla and D. Garfinkle, *Class. Quantum Gravity* **32**, 124008 (2015).
14. Y. Choquet-Bruhat, *General Relativity and the Einstein Equations* (Oxford University Press, 2009).
15. N. D. Birrel and P. C. W. Davies, *Quantum Fields in Curved Space* (Cambridge University Press, Cambridge, England, 1984).
16. R. M. Wald, *Living Rev. Relativ.* **4**, 6 (2001).
17. T. A. Roman and P. G. Bergman, *Phys. Rev. D* **28**, 1265 (1983).
18. S. A. Hayward, *Phys. Rev. Lett.* **96**, 031103 (2006).
19. J. W. York, Jr., *Phys. Rev. D* **28**, 2929 (1983).
20. G. Abreu and M. Visser, *Phys. Rev. D* **82**, 044027 (2010).
21. C. W. Misner and D. H. Sharp, *Phys. Rev.* **136**, B571 (1964).
22. V. Faraoni, G. F. R. Ellis, J. T. Firouzjaee, A. Helou, and I. Musco, *Phys. Rev. D* **95**, 024008 (2017).
23. R. Penrose, *Structure of space-time*, in C. DeWitt, J. A. Wheeler (eds.), *Batelle Rencontres: 1967 Lectures in Mathematics and Physics*, pp. 121–235 (W. A. Benjamin, San Francisco, 1968).

24. F. J. Tipler, C. J. S. Clarke, and G. R. F. Ellis, *Singularities and horizons: a review article*, in A. Held A (ed.), *General relativity and gravitation: one hundred years after the birth of Albert Einstein*, vol. 2, p. 97 (Plenum, New York, 1980).
25. H. Stephani, D. Kramer, M. MacCallum, C. Hoenselaers, and E. Herlt, *Exact Solutions of Einstein's Field Equations*, 2nd ed. (Cambridge University Press, Cambridge, 2003).
26. D. R. Terno, *Phys. Rev. D* **100**, 124025 (2019).
27. V. Baccetti, R. B. Mann, S. Murk, and D. R. Terno, *Phys. Rev. D* **99**, 124014 (2019).
28. D. R. Terno, *Phys. Rev. D* **101**, 124053 (2020).
29. S. Murk and D. R. Terno, *Phys. Rev. D* **103**, 064082 (2021).
30. P. Martín-Moruno and M. Visser, *Classical and Semi-classical Energy Conditions*, in *Wormholes, Warp Drives and Energy Conditions*, edited by F. N. S. Lobo (Springer, New York, 2017), p. 193.
31. E.-A. Kontou and K. Sanders, *Class. Quantum Gravity* **37**, 193001 (2020).
32. V. Baccetti, S. Murk, and D. R. Terno, *Phys. Rev. D* **100**, 064054 (2019).
33. W. G. Unruh, *Phys. Rev. D* **14**, 870 (1976).
34. M. Visser, *Phys. Rev. D* **56**, 936 (1997).
35. A. Levi and A. Ori, *Phys. Rev. Lett.* **117**, 231101 (2016).
36. C. J. Fewster, *Quantum Energy Inequalities*, in *Wormholes, Warp Drives and Energy Conditions*, edited by F. N. S. Lobo (Springer, New York, 2017), p. 215.
37. E.-A. Kontou and K. D. Olum, *Phys. Rev. D* **91**, 104005 (2015).
38. P. K. Dahal, S. Murk, and D. R. Terno, arXiv:2110.00722 (2021).
39. R. B. Mann, S. Murk, and D. R. Terno, arXiv:2109.13939 (2021).
40. G. F. R. Ellis and A. R. King, *Commun. Math. Phys.* **38**, 119 (1974).
41. B. Cropp, S. Liberati, and M. Visser, *Class. Quantum Gravity* **30**, 125001 (2013).
42. P. Hájíček, *Phys. Rev. D* **36**, 1065 (1987).
43. C. Barceló, S. Liberati, S. Sonego, and M. Visser, *Class. Quantum Gravity* **23**, 5341 (2006).
44. T. Vachaspati, D. Stojkovic, and L. M. Krauss, *Phys. Rev. D* **76**, 024005 (2007).
45. A. Paranjape and T. Padmanabhan, *Phys. Rev. D* **80**, 044011 (2009).
46. C. Barceló, S. Liberati, S. Sonego, and M. Visser, *Phys. Rev. D* **83**, 041501(R) (2011).
47. F. Kurpicz, N. Pinamonti, and R. Verch, arXiv:2102.11547 (2021).
48. S. A. Hayward, *Class. Quantum Gravity* **15**, 3147 (1998).
49. P. K. Dahal and D. R. Terno, *Phys. Rev. D* **102**, 124032 (2020).
50. D. N. Page, *Phys. Rev. D* **13**, 198 (1976).